Langmuir
Article
pubs.acs.org/Langmuir

Highlighting a Variety of Unusual Characteristics of Adsorption and Diffusion in Microporous Materials Induced by Clustering of Guest Molecules

Rajamani Krishna* and Jasper M. van Baten

Van 't Hoff Institute for Molecular Sciences, University of Amsterdam, Nieuwe Achtergracht 166, 1018 WV Amsterdam, The Netherlands

Received December 29, 2009. Revised Manuscript Received February 11, 2010

In this work, we highlight several unusual characteristics of adsorption and diffusion of a variety of guest molecules, such as linear and branched alkanes with a number of C atoms in the 1−6 range, CO_2, and Ar in microporous structures such as zeolites (FAU, NaY) and metal organic frameworks (IRMOF-1, CuBTC, MIL-47, MIL-53 (Cr)-lp, PCN-6′) that have channel or cavity sizes larger than about 0.75 nm. Clustering of guest molecules is found to manifest at temperatures below the critical temperature, T_c, of the guest species. The degree of clustering is increased as the temperature, T, is reduced increasingly below T_c. For linear alkanes, T_c increases with chain length and, consequently, at a given T the degree of clustering increases with increasing chain length. For C4, C5, and C6 alkane isomers, the linear isomer shows a higher degree of clustering than the corresponding branched isomers. Mixture adsorption characteristics are significantly influenced by clustering; specifically, the separation selectivity is found to increased significantly with lowering T. We also discuss the interesting possibility of separating alkane isomer mixtures by exploiting the differences in the degrees of clustering, induced by differences in T_c of constituent species. An important characteristic of clustering is that the inverse thermodynamic factor $1/\Gamma_i \equiv (\mathrm{d}\ln c_i)/(\mathrm{d}\ln f_i)$ exceeds unity for a range of molar concentrations c_i within the micropores. For the concentration ranges for which $1/\Gamma_i > 1$, the Fick diffusivity, D_i, for unary diffusion is often lower than both the Maxwell-Stefan, $Đ_i$, and the self-diffusivity, $D_{i,\mathrm{self}}$. Correlation effects in diffusion are significantly lowered as a consequence of clustering; this reduction in correlation effects is found to have a significant influence on the mixture diffusion characteristics. The diffusion selectivity is significantly affected with increased clustering.

1. Introduction

Microporous structures such as zeolites and metal organic frameworks (MOFs) are used in a variety of storage, separation, and reaction applications.[1−11] In the development of all such applications, it is essential to have proper insights, along with a good quantitative description of the adsorption of guest molecules.[9−16] Additionally, in some applications such as membrane separations and catalysis, it is also necessary to have a proper quantitative description of mixture diffusion within the micropores.[11,15−21] Depending on the process application, the chosen operating temperature T can be either higher or lower than the critical temperature, T_c, of the constituent species.

In our previous work,[22] it was shown that for adsorption of CO_2 ($T_c = 304$ K), CH_4 ($T_c = 191$ K), and Ar ($T_c = 151$ K) below their respective critical temperatures T_c, clustering of molecules occurs in zeolites, metal-organic frameworks (MOFs), and covalent-organic frameworks (COFs), that have characteristic channel or cavity dimensions larger than about 0.75 nm. Clustering was found to be severe in "open structures" such as CuBTC, IRMOF-1, COF-102, and COF-108 with pore volumes, $V_p = 0.85$, 1.37, 1.88, and 5.5 $\mathrm{cm^3/g}$, respectively. We had shown that, in regions where clustering occurs, the inverse thermodynamic factor, $1/\Gamma_i$, defined by

$$\frac{1}{\Gamma_i} \equiv \frac{\partial \ln c_i}{\partial \ln f_i} = \frac{f_i \partial c_i}{c_i \partial f_i} \tag{1}$$

exceeds unity, and the concentration dependences of the Maxwell-Stefan (M-S) diffusivity, $Đ_i$, and Fick diffusivity, D_i, are significantly influenced.

In many separation and reaction applications utilizing zeolites and MOFs, larger molecules such as alkanes and aromatics are encountered. The critical temperatures of these molecules are often higher than the operating temperatures, and the question

*Corresponding author. Tel: +31 20 257007; Fax: + 31 20 5255604; e-mail: r.krishna@uva.nl.

(1) Kärger, J.; Ruthven, D. M. *Diffusion in zeolites and other microporous solids*; John Wiley: New York, 1992.
(2) Férey, G. *Chem. Soc. Rev.* **2008**, *37*, 191–214.
(3) Férey, G.; Serre, C. *Chem. Soc. Rev.* **2009**, *38*, 1380–1399.
(4) Li, J. R.; Kuppler, R. J.; Zhou, H. C. *Chem. Soc. Rev.* **2009**, *38*, 1477–1504.
(5) Murray, L. J.; Dincă, M.; Long, J. R. *Chem. Soc. Rev.* **2009**, *38*, 1294–1314.
(6) Lee, J. Y.; Farha, O. K.; Roberts, J.; Scheidt, K. A.; Nguyen, S. T.; Hupp, J. T. *Chem. Soc. Rev.* **2009**, *38*, 1450–14594.
(7) Czaja, A. U.; Trukhan, N.; Müller, U. *Chem. Soc. Rev.* **2009**, *38*, 1284–1293.
(8) Düren, T.; Bae, Y. S.; Snurr, R. Q. *Chem. Soc. Rev.* **2009**, *38*, 1237–1247.
(9) Krishna, R.; Paschek, D. *Sep. Purif. Technol.* **2000**, *21*, 111–136.
(10) Krishna, R.; Baur, R. *Sep. Purif. Technol.* **2003**, *33*, 213–254.
(11) Hansen, N.; Krishna, R.; van Baten, J. M.; Bell, A. T.; Keil, F. J. *J. Phys. Chem. C* **2009**, *113*, 235–246.
(12) Jiang, J.; Sandler, S. I. *Langmuir* **2006**, *22*, 5702–5707.
(13) Smit, B.; Maesen, T. L. M. *Chem. Rev.* **2008**, *108*, 4125–4184.
(14) Castillo, J. M.; Vlugt, T. J. H.; Calero, S. *J. Phys. Chem. C* **2009**, *113*, 20869–20874.
(15) Keskin, S.; Liu, J.; Rankin, R. B.; Johnson, J. K.; Sholl, D. S. *Ind. Eng. Chem. Res.* **2009**, *48*, 2355–2371.
(16) Krishna, R. *J. Phys. Chem. C* **2009**, *113*, 19756–19781.
(17) Keskin, S.; Sholl, D. S. *J. Phys. Chem. C* **2007**, *111*, 14055–14059.
(18) Keskin, S.; Sholl, D. S. *Ind. Eng. Chem. Res.* **2009**, *48*, 914–922.
(19) Keskin, S.; Sholl, D. S. *Langmuir* **2009**, *25*, 11786–11795.
(20) Babarao, R.; Jiang, J. *Langmuir* **2008**, *24*, 5474–5484.
(21) Babarao, R.; Tong, Y. H.; Jiang, J. *J. Phys. Chem. B* **2009**, *113*, 9129–9136.
(22) Krishna, R.; van Baten, J. M. *Langmuir* **2010**; http://dx.doi.org/10.1021/la9033639.

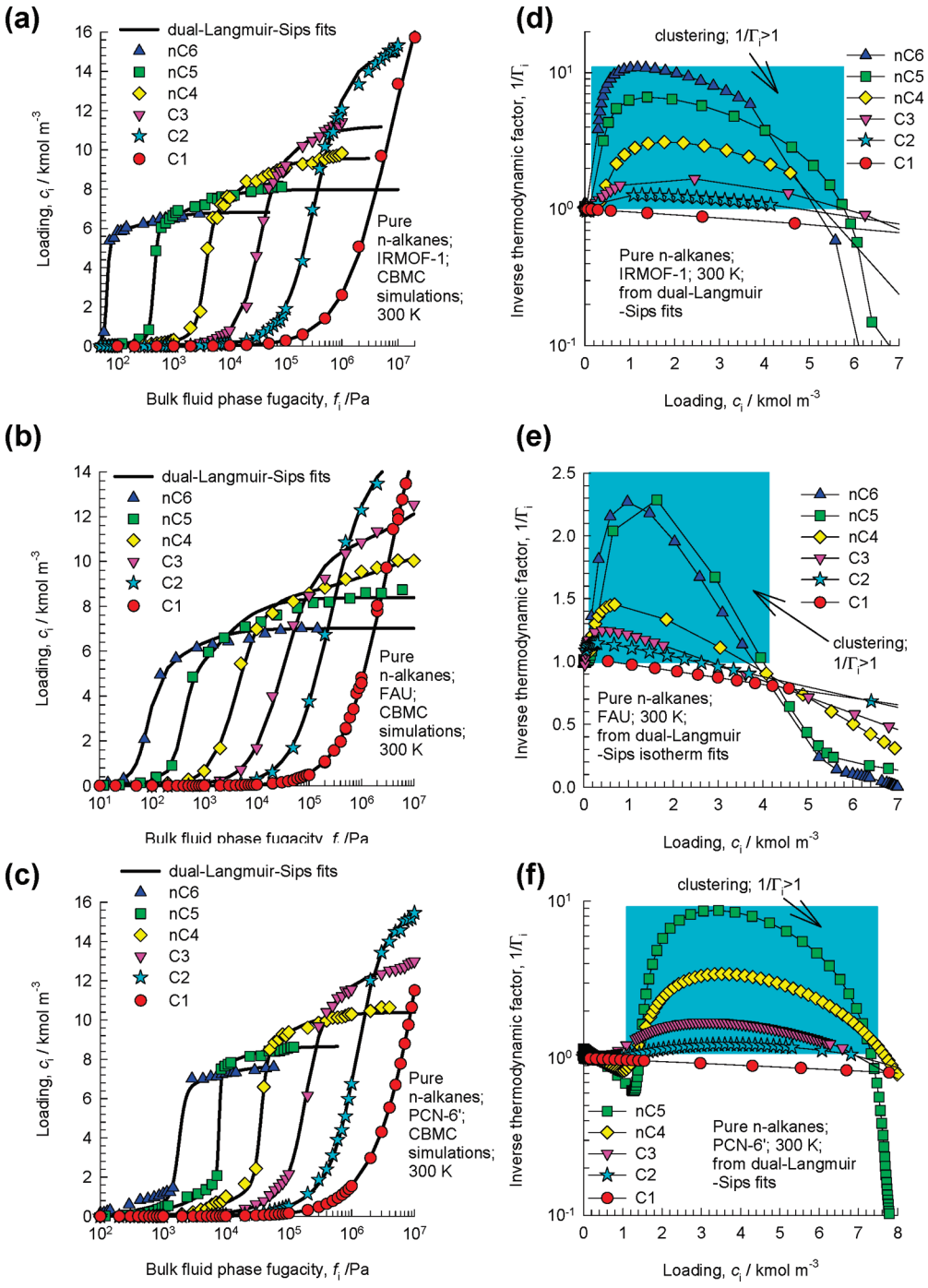

Figure 1. (a,b,c) CBMC simulations of adsorption isotherms for *n*-alkanes in IRMOF-1, FAU, and PCN-6′ at 300 K. Also shown with the continuous solid lines are the dual-Langmuir-Sips fits of the isotherms. (d,e,f) The inverse thermodynamic factor, $1/\Gamma_i$, plotted as a function of the pore loading, c_i, for *n*-alkanes in IRMOF-1, FAU, and PCN-6′. The $1/\Gamma_i$ is calculated by differentiation of dual-Langmuir-Sips fits of the isotherms shown in (a,b,c).

arises whether molecular clustering occurs in such cases too. Consider, for example, the adsorption of alkanes with the number of C atoms in the range 1−6 within microporous host structures. For adsorption at 300 K, except for CH_4 (C1), the chosen operating temperature is below the critical temperatures of the higher alkanes: ethane (C2, T_c = 305 K), propane (C3, T_c = 370 K), *n*-butane (nC4, T_c = 425 K), 2-methylpropane (iC4, T_c = 408 K), n-pentane (nC5, T_c = 470 K), 2-methylbutane (2MB, T_c = 460 K), 2,2-dimethylpropane (neo-C5, T_c = 434 K), *n*-hexane (nC6, T_c = 507.4 K), 3-methylpentane (3MP, T_c = 504.4 K), and 2,2-dimethylbutane (22DMB, T_c = 488.7 K). In the investigation of Jiang and Sandler[12] on adsorption of linear and branched alkanes with varying C numbers in IRMOF-1 at 300 K, the adsorption isotherms for C2, C3, nC4, nC5, 2MB, and neo-C5 show the stepped characteristic typical of adsorption of CO_2, and CH_4 in IRMOF-1 and COFs at subcritical temperatures.[22−25] Furthermore, the radial distribution functions for nC5 show clear

(23) Walton, K. S.; Millward, A. R.; Dubbeldam, D.; Frost, H.; Low, J. J.; Yaghi, O. M.; Snurr, R. Q. *J. Am. Chem. Soc.* **2008**, *130*, 406–407.
(24) Yang, Q.; Zhong, C. *Langmuir* **2009**, *25*, 2302–2308.
(25) Ma, Q.; Yang, Q.; Zhong, C.; Mi, J.; Liu, D. *Langmuir* **2009**; http://dx.doi.org/10.1021/la903643f.

evidence of molecular clustering, even though this aspect was not highlighted by Jiang and Sandler.[12] Babarao et al.[21] report similar stepped isotherm characteristics for a variety of alkanes in IRMOF-13, IRMOF-14, PCN-6′, and PCN-6. Several questions arise on the basis of these two investigations. If indeed cluster formation occurs for alkanes with two or more C atoms, what is the corresponding influence on the inverse thermodynamic factor $1/\Gamma_i$? What is the corresponding influence on the concentration dependences of the diffusivities of alkanes? In the investigation of Chmelik et al.,[26] using infrared microscopy experiments supplemented with molecular simulations of adsorption and diffusion of alkanes in CuBTC, it was shown that, in regions where $1/\Gamma_i$ exceeds unity, the Fick diffusivity of 2MB and neo-C5 exhibits a sharp minimum. Is this minimum a direct consequence of clustering? Should we expect similar behavior for alkanes diffusion in IRMOF-1, and also in other open structures?

The influence of molecular clustering on adsorption and diffusion of mixtures also deserves investigation. In the work of Babarao et al.,[21] the adsorption and diffusion of mixtures of nC4 and iC4 in PCN-6′ and PCN-6 have been investigated for a temperature of 300 K, significantly lower than the critical temperature of either species. The self-diffusivities in the binary nC4-iC4 mixtures show curious maxima at a certain mixture loading. In addition to the explanations provided by Babarao et al.,[21] we could ask the question whether molecular clustering contributes to the curious maxima reported by these authors?

Babarao et al.[21] also investigated the adsorption of C4 and C5 isomer mixtures and found selectivities in favor of the linear isomer, that they attribute to "configurational entropy effects". Can the principle be extended to separate C6 isomers?

In the current work, we seek answers to the questions posed above. Furthermore, we aim to provide a broader perspective on the influence of clustering on adsorption and diffusion of mixtures in microporous structures. Specifically, our work has the following set of objectives: (1) to demonstrate that clustering phenomena also manifests for alkanes when operating below the critical temperatures (for this purpose, we investigate the adsorption and diffusion of linear and branched alkanes up to 6 C atoms in "open" structures such as IRMOF-1, FAU, and PCN-6′; we aim to highlight unusual concentration dependences, and hierarchy of values, of M-S, Fick, and self-diffusivities); (2) to investigate the influence of molecular clustering on correlation effects in diffusion of single components and binary mixtures in a variety of microporous materials (we aim to show that molecular clustering has the effect of reducing correlation effects to a significant extent); (3) to investigate the influence of varying T, below and above T_c, on diffusivities of a variety of guest molecules (we aim to show that the activation energies of the self- and M-S diffusivities are not the same; differences arise to the variation in the degree of clustering with varying T); (4) to show that molecular clustering has a significant influence on the selectivity of adsorption and diffusion of mixtures (for this purpose, we investigate adsorption of a variety of binary mixtures in IRMOF-1, MIL-47, MIL-53 (Cr), FAU, CuBTC, and PCN-6′).

To achieve the aforementioned objectives, we use Configurational-Bias Monte Carlo (CBMC) simulations of adsorption isotherms in the grand canonical ensemble, along with molecular dynamics (MD) simulations of diffusivities of pure components and mixtures.

The entire database of simulation results is available in the Supporting Information accompanying this publication; this material includes details of the CBMC and MD simulation methodologies, details of the microporous structures (unit cell dimensions, accessible pore volume, characteristic pore dimensions), pore landscapes, specification of the force fields used, simulation data on isotherms, clustering analysis, and diffusivities.

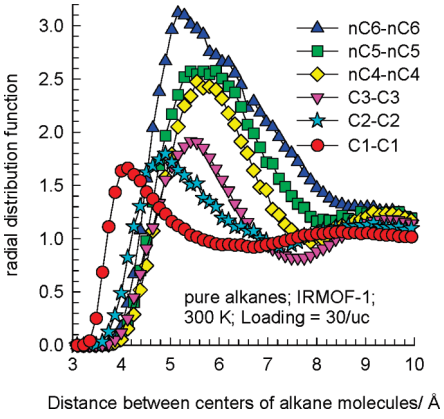

Figure 2. Radial distribution function (RDF) for adsorption of *n*-alkanes in IRMOF-1 at 300 K for a loading of 30 molecules per unit cell, corresponding to $c_i = 3.56$ kmol m^{-3}. The RDF is constructed on the basis of the distances between the centers of mass of molecules.

2. Cluster Formation in Adsorption of Alkanes

Figure 1a,b,c show the CBMC simulations of pure component isotherms for linear alkanes: methane (CH_4), C2, C3, nC4, nC5, and nC6 at 300 K in IRMOF-1, FAU, and PCN-6′. The c_i values are the absolute loadings, expressed as the number of moles per cubic meter of *accessible* pore volume; this allows a proper comparison of the loadings in different structures; this choice of concentration measure is useful not only for modeling adsorption, but also for diffusion.[16,21,22,27,28] The accessible pore volumes of the variety of structures investigated were determined with the aid of molecular simulations using the helium probe insertion technique suggested by Talu and Myers.[29,30] With increasing chain length, the critical temperature increases, and the isotherms become progressively steeper. The continuous solid lines in Figure 1a,b,c are fits using the dual-Langmuir-Sips isotherm[22,26]

$$c_i = c_{i,A,\mathrm{sat}} \frac{b_{i,A} f_i^{\nu_{i,A}}}{1 + b_{i,A} f_i^{\nu_{i,A}}} + c_{i,B,\mathrm{sat}} \frac{b_{i,B} f_i^{\nu_{i,B}}}{1 + b_{i,B} f_i^{\nu_{i,B}}} \qquad (2)$$

All six constants in eq 2 were fitted to match the CBMC simulated isotherms; neither exponent $\nu_{i,A}$ nor $\nu_{i,B}$ was restricted to unity. The inverse thermodynamic factor, $1/\Gamma_i$, can be obtained by analytic differentiation of eq 2. The data for $1/\Gamma_i$ are presented in Figure 1d,e,f. We prefer to plot $1/\Gamma_i$ instead of Γ_i because the latter has the undesirable property of approaching infinity as saturation loading is approached; this makes the data less easy to interpret when plotted in graphical form. For a single-site Langmuir isotherm, we have $1/\Gamma_i = (1 - \theta_i) = (1 - c_i/c_{i,\mathrm{sat}})$, i.e., the fractional vacancy. We note that $1/\Gamma_i$ exceeds unity to increasing extents as the chain length increases. In previous work,[22] we had argued that the condition $1/\Gamma_i > 1$ implies the increase of fractional vacancy beyond unity and this is physically rationalized if we allow for molecular clustering. As discussed in detail in our previous work,

(26) Chmelik, C.; Kärger, J.; Wiebcke, M.; Caro, J.; van Baten, J. M.; Krishna, R. *Microporous Mesoporous Mater.* **2009**, *117*, 22–32.

(27) Krishna, R.; van Baten, J. M. *Chem. Eng. Sci.* **2009**, *64*, 870–882.
(28) Krishna, R.; van Baten, J. M. *Chem. Eng. Sci.* **2009**, *64*, 3159–3178.
(29) Talu, O.; Myers, A. L. *A. I. Ch. E. J.* **2001**, *47*, 1160–1168.
(30) Myers, A. L.; Monson, P. A. *Langmuir* **2002**, *18*, 10261–10273.

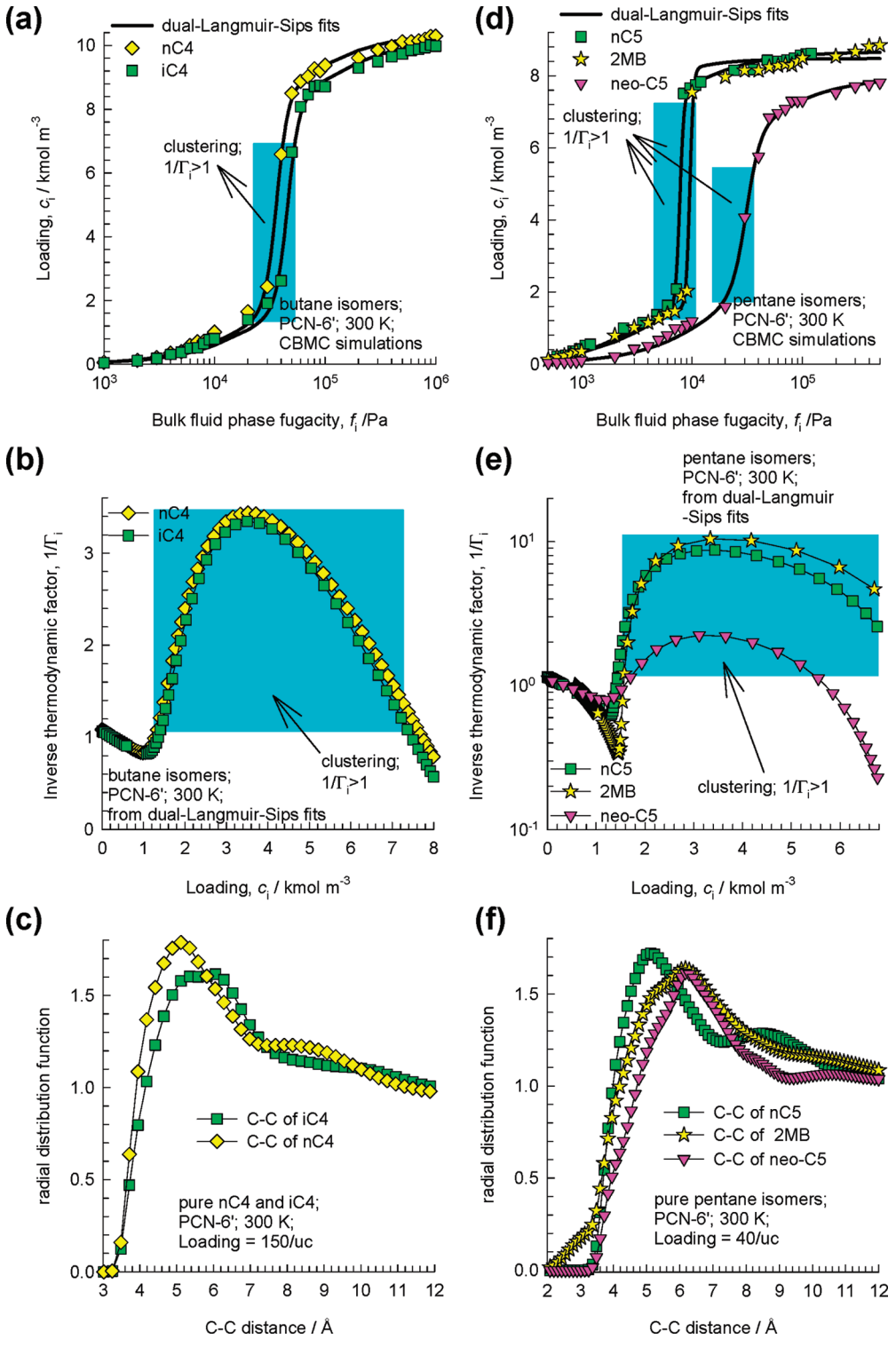

Figure 3. (a,d) CBMC simulations of adsorption isotherms for butane (nC4, and iC4) and pentane (nC5, 2MB, and neo-C5) isomers in PCN-6′ at 300 K. Also shown with the continuous solid lines are the dual-Langmuir-Sips fits of the isotherms. (b,e) The inverse thermodynamic factor, $1/\Gamma_i$, plotted as a function of the pore loading, c_i. The $1/\Gamma_i$ is calculated by differentiation of dual-Langmuir-Sips fits of the isotherms. (c,f) Radial distribution function (RDF) for a loading of 150 molecules per unit cell, corresponding to $c_i = 2.72$ kmol m^{-3}. Here, the RDF is constructed based on the distances between intermolecular C−C atoms, and not between the centers of mass.

we also confirmed that the concentration ranges for which $1/\Gamma_i > 1$ falls within the bimodal phase envelope of the alkane. The data in Figure 1 imply that molecular clustering increases with increasing chain length. To verify this and further quantify the degree of clustering, we calculated the radial distribution functions (RDF) for *n*-alkanes in IRMOF-1 at 300 K for a loading of 30 molecules per unit cell, corresponding to $c_i = 3.56$ kmol m^{-3}; the results are shown in Figure 2. We note that, with increasing chain length, the peak in the RDF is higher, indicating a higher degree of clustering. Put another way, the trends in $1/\Gamma_i$ observed in Figure 1 are in line with the RDFs in Figure 2. Increased clustering with increasing chain length leads to steeper isotherms and higher $1/\Gamma_i$ values. The

results presented in Figure 2 are in line with previous work[22] in which we showed that the degree of clustering increases as the reduced temperature, $T_R = T/T_c$, falls to increasing extents below unity. For the data for *n*-alkanes presented in Figure 2, T_R decreases progressively from 1.57 for CH_4 to a value of 0.59 for nC6. In subsequent discussions, we shall interpret the condition $1/\Gamma_i > 1$ to be synonymous with clustering of molecules within that loading c_i range.

We now compare the adsorption characteristics of alkane isomers. Consider the adsorption of nC4 and iC4 in PCN-6′. For adsorption at 300 K, the reduced temperatures are $T_R = 0.705$ and 0.735. As a consequence, the isotherm of nC4 is steeper (cf. Figure 3a), has a higher value of $1/\Gamma_i$ (cf. Figure 3b), and exhibits a higher degree of clustering as witnessed by a higher peak in the RDF (cf. Figure 3c). Particularly noteworthy is the $1/\Gamma_i$ vs c_i characteristic that shows an initial decline below unity for the range $0 < c_i < 1.2$ kmol m^{-3}. This decline is due to the fact that the C4 isomers are located preferentially in the octahedral pockets, as pointed out by Babarao et al.[21] For the higher loading range $1.2 < c_i < 7$ kmol m^{-3}, the more open spaces of PCN-6′ become populated.

The corresponding results for adsorption nC5, 2MB, and neo-C5 in PCN-6′ are presented in Figure 3d,e,f. For adsorption at 300 K, the reduced temperatures are $T_R = 0.64$, 0.65, and 0.69. Consequently, neo-C5 experiences the lowest degree of clustering, as evidenced both by $1/\Gamma_i$ and the RDFs. As in the case of C4 isomers, the C5 isomers too are located preferentially in the octahedral pockets for loadings $c_i < 1.5$. The minimum in $1/\Gamma_i$ for low concentration ranges is exactly analogous to the minimum observed by Chmelik et al.[26] for alkane adsorption in CuBTC, caused by the preferential location within the tetrahedral pockets. The minimum value of $1/\Gamma_i$ is particularly prominent for 2MB, and this suggests that the octahedral pockets of PCN-6′ are particularly favorable locations for 2MB. This preferential location also gets reflected in the RDF for 2MB, which shows a linear step in the 2−4 Å range for separation distances.

Analogous results to those presented in Figure 3 are obtained for adsorption of C4 and C5 isomers in IRMOF-1; details are provided in the Supporting Information. There are no pocket regions in IRMOF-1, and therefore the initial decline in $1/\Gamma_i$ below unity is not encountered.

3. Influence of Clustering on Adsorption Selectivity of Mixtures

Figure 4a presents data on the influence of temperature on the adsorption selectivity of CH_4(1)-CO_2(2) mixtures in IRMOF-1. We note that selectivity is higher as the temperature is increasingly lowered below 300 K. This is because at any $T < 300$ K, the degree of clustering of CO_2 is higher than that of CH_4. A higher degree of clustering results in stronger adsorption of that component. We also note from Figure 4a that even at low loadings there is a significant influence of T on selectivity; this is due to differences in the adsorbate−adsorbent binding energies for the two constituents. Results similar to that for IRMOF-1, were obtained for CH_4(1)-CO_2(2) adsorption in several other host structures; see data in Supporting Information. A similar result is also obtained for CH_4(1)-C3(2) mixtures in IRMOF-1; see Figure 4b. A lower temperature results in a higher selectivity toward propane due to stronger clustering. If T is sufficiently high, the adsorption selectivity becomes almost insensitive to T, as shown by Yang et al.[31] for CO_2/N_2 mixture adsorption in CuBTC.

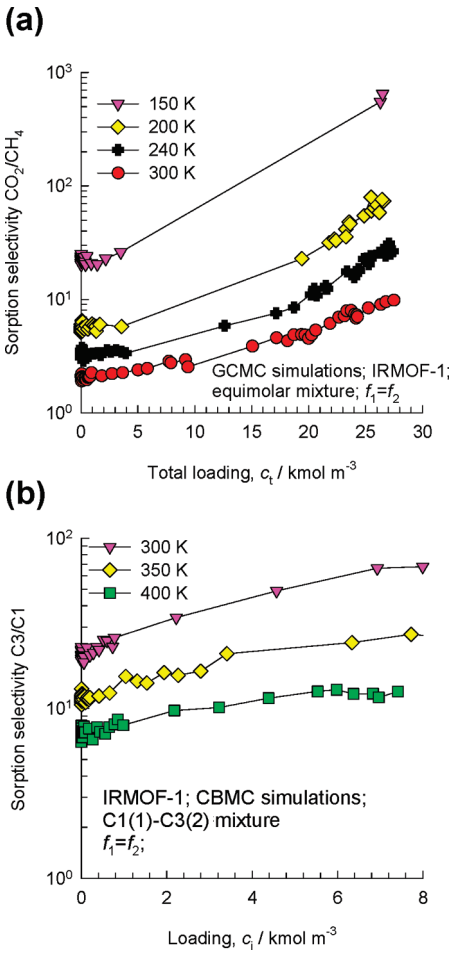

Figure 4. Influence of temperature on the adsorption selectivity of (a) CH_4(1)-CO_2(2), and (b) CH_4(1)-C3(2) mixtures in IRMOF-1. The partial fugacities in the bulk fluid phase of the components are taken to be equal, i.e., $f_1 = f_2$.

The foregoing results suggest the possibility of separating alkane isomers mixtures based on differences in the degree of clustering. To illustrate this, we performed CBMC simulations for adsorption of nC4/iC4, nC5/2MB/neo-C5, and nC6/3MP/22DMB mixtures in both IRMOF-1 and PCN-6′; the results are presented in Figure 5. For all three mixtures, the adsorption selectivity is strongly in favor of the linear isomer. The hierarchy of component loadings is dictated by the hierarchy in the values of T_c, leading us to conclude that the root cause of the separation is based on differences in the degrees of clustering of constituent species. Linear alkanes can "stack" more easily. When, for example, hexane isomers are cooled, the first crystals to form will be that of nC6, that has the highest freezing point. The same principle applies to clustering. Ease of crystal formation translates to a higher propensity to form clusters. Conversely, molecules such as neo-C5 and 22DMB do not stack as efficiently as the linear isomers, and consequently have more difficulty in forming clusters, and also have to be cooled to much lower temperatures to form crystals.[32] In this context, it is appropriate to state that Jiang and Sandler[12] and Babarao et al.[21] were the first to report a similar preferential adsorption selectivity toward the linear isomers nC4 and nC5 in IRMOF-1 and in PCN-6′ and have attributed this to "configurational entropy

(31) Yang, Q.; Xue, C.; Zhong, C.; Chen, J. F. *A. I. Ch. E. J.* **2007**, *53*, 2832–2840.

(32) Schenk, M.; Vidal, S. L.; Vlugt, T. J. H.; Smit, B.; Krishna, R. *Langmuir* **2001**, *17*, 1558–1570.

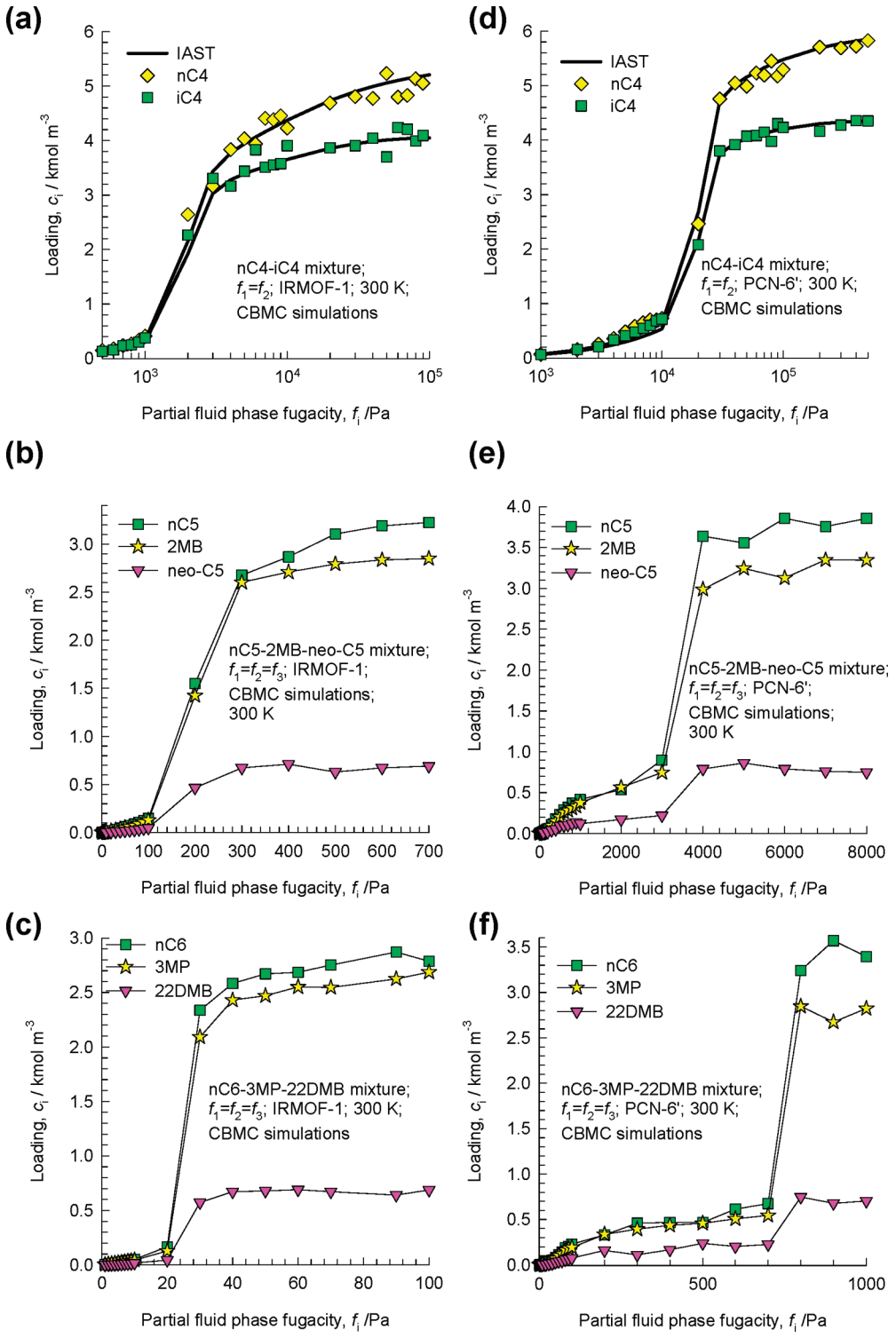

Figure 5. CBMC simulations of adsorption isotherms for (a,d) nC4/C4 and (b,e) nC5/2MB/neo-C5, and (c,f) nC6/3MP/22DMB mixtures in (a,b,c) IRMOF-1 and (d,e,f) PCN-6′ at 300 K. The partial fugacities in the bulk fluid phase of the components are taken to be equal, i.e., $f_1 = f_2 = f_3$. Also shown with the continuous solid lines for nC4/iC4 mixtures are the estimations of component loadings using the ideal adsorbed solution theory (IAST) of Myers and Prausnitz[51] using the dual-Langmuir-Sips fits of the pure component isotherms.

effects", drawing parallels with the principles used to separate alkane isomers in zeolites such as MFI, MOR, and AFI in which the molecules are more strongly confined.[32−34] Indeed, our investigations have shown that differences in the packing efficiencies of alkane isomers, cause differences in clustering and therefore adsorptivities.

Gu et al.[35] have presented experimental data on separation of mixtures of *o*-xylene (T_c = 418 K), *m*-xylene (T_c = 412.3 K),

(33) Krishna, R.; Smit, B.; Calero, S. *Chem. Soc. Rev.* **2002**, *31*, 185–194.
(34) Vlugt, T. J. H.; Krishna, R.; Smit, B. *J. Phys. Chem. B* **1999**, *103*, 1102–1118.
(35) Gu, Z. Y.; Jiang, D. Q.; Wang, H. F.; Cui, X. Y.; Yan, X. P. *J. Phys. Chem. C* **2010**, *114*, 311–316.

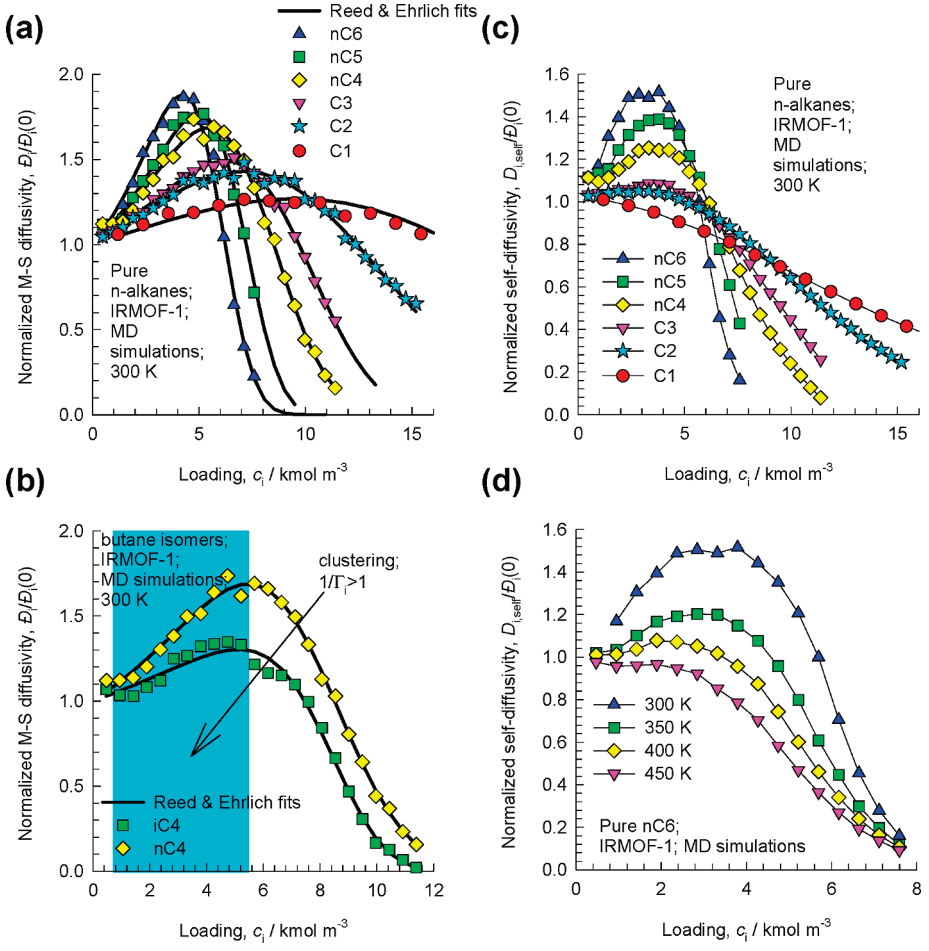

Figure 6. (a,b) Normalized M-S diffusivities $Đ_i/Đ_i(0)$ for (a) *n*-alkanes, and (b) C4 isomers in IRMOF-1 at 300 K. The continuous solid lines are the fits using the Reed and Ehrlich model for the loading dependence of $Đ_i$.[40,52] (c) Normalized self-diffusivities $D_{i,\text{self}}/Đ_i(0)$ for *n*-alkanes in IRMOF-1 at 300 K. (d) Comparison of normalized self-diffusivities $D_{i,\text{self}}/Đ_i(0)$ for nC6 in IRMOF-1 at 300 K, 350 K, 400 K, and 450 K.

p-xylene (T_c = 411.5 K), and ethylbenzene (T_c = 409.3 K) using IRMOF-1. Ethylbenzene has the poorest adsorption selectivity, and a likely explanation is its lowest degree of clustering.

In a simulation study, Castillo et al.[14] have demonstrated the potential of using MIL-47 to separate xylene isomers at $T = 343$ K. Their simulations show separation selectivities in favor of *o*-xylene, that has the highest T_c and consequently the highest propensity to form clusters.

4. Influence of Molecular Clustering on Diffusion Characteristics

Consider first the loading dependence of the M-S diffusivity, $Đ_i$, of *n*-alkanes. Figure 6a presents the data, normalized with respect to the zero-loading value, $Đ_i/Đ_i(0)$, for *n*-alkanes in IRMOF-1 at 300 K. For low concentration ranges, we note that $Đ_i/Đ_i(0)$ increases to increasingly sharper extents with chain length, synchronous with the corresponding $1/\Gamma_i$ behavior portrayed in Figure 1. As $1/\Gamma_i$ is a measure of the fractional vacancy, the physical reasoning behind the increase of $Đ_i/Đ_i(0)$ is the increase in the availability of vacant sites due to molecular clustering. The maximum in the normalized diffusivities occur within the concentration ranges for which the corresponding $1/\Gamma_i$ exceeds unity (cf. Figure 1). For alkane isomers, the linear isomer exhibits a sharper increase in the $Đ_i$ as a direct consequence of clustering; see diffusivity data for C4 isomers in IRMOF-1 in Figure 6b.

MD simulations on diffusivities of methanol in NaY and NaX display a maximum for a range of concentrations.[36,37] The root cause of this maximum can be traced to dimer formation, and so must be considered to be analogous to the results of Figures 6.

It noteworthy that the $Đ_i$ vs c_i behavior of the M-S diffusivity of a variety of guest species has been shown to exhibit a similar maximum in microporous structures such LTA, CHA, DDR, and ERI that consist of cages separated by narrow windows.[38−41] However, in these cases, the $Đ_i$ vs c_i is governed by the alteration in the free energy barrier for hopping across the narrow windows.

We now examine how clustering influences the hierarchy of values of the M-S, Fick, and self- diffusivities. Following the M-S formulation of unary diffusion,[16] the self-diffusivity, $D_{i,\text{self}}$, is related to the M-S diffusivity $Đ_i$, by

$$\frac{1}{D_{i,\text{self}}} = \frac{1}{Đ_i} + \frac{1}{Đ_{ii}} \tag{3}$$

At any pore loading, the self-diffusivity $D_{i,\text{self}}$ is lower than the M-S diffusivity $Đ_i$; this is because individual jumps of molecules

(36) Plant, D. F.; Maurin, G.; Bell, R. G. *J. Phys. Chem. B* **2006**, *110*, 15926–15931.
(37) Nanok, T.; Vasenkov, S.; Keil, F.; Fritzsche, S. *Microporous Mesoporous Mater.* **2010**, *127*, 176–181.
(38) Beerdsen, E.; Dubbeldam, D.; Smit, B. *Phys. Rev. Lett.* **2005**, *95*, 164505.
(39) Beerdsen, E.; Dubbeldam, D.; Smit, B. *Phys. Rev. Lett.* **2006**, *96*, 044501.
(40) Krishna, R.; van Baten, J. M. *Microporous Mesoporous Mater.* **2008**, *109*, 91–108.
(41) Krishna, R.; van Baten, J. M. *Chem. Eng. Sci.* **2008**, *63*, 3120–3140.

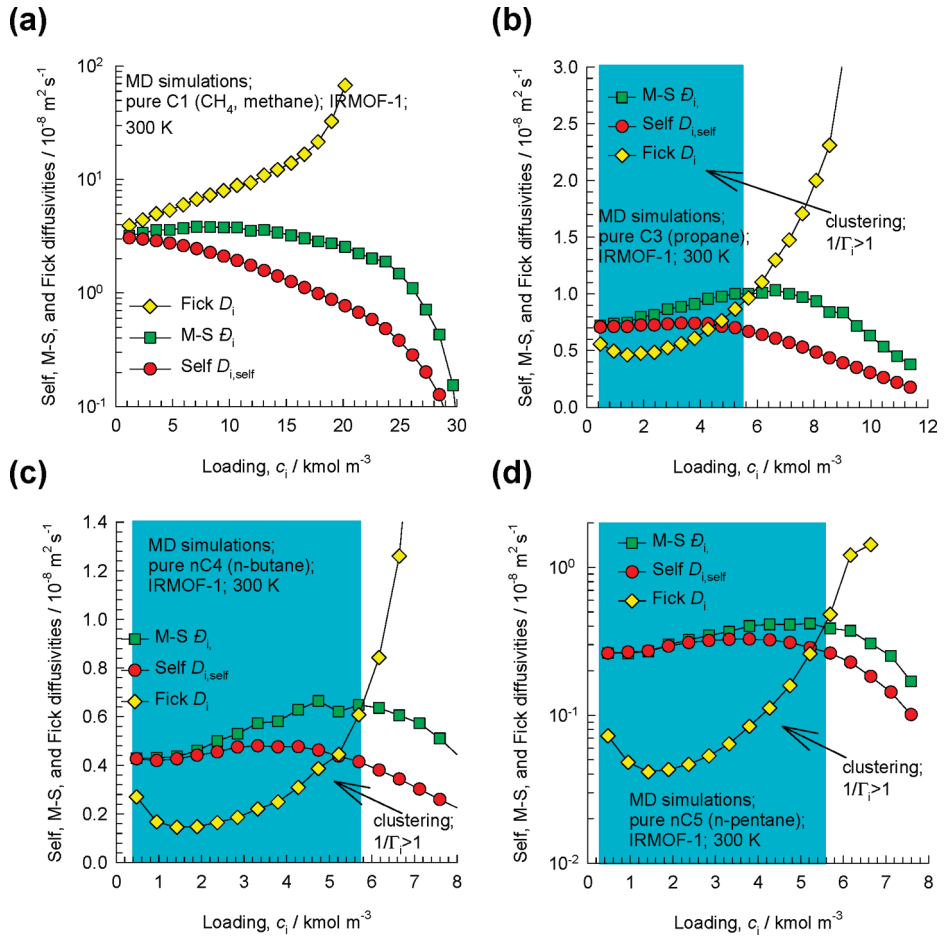

Figure 7. The loading dependences of the Maxwell-Stefan (M-S) diffusivity, $Đ_i$, Fick diffusivity, D_i, and the self-diffusivity, $D_{i,self}$ for (a) CH_4, (b) C3, (c) nC4, and (d) nC5 in IRMOF-1 at 300 K.

are *correlated* due to revisitation of sites that have been recently abandoned. The $Đ_i$, reflecting *collective* motion of molecules, is free from such correlation effects; it is for this reason that the $Đ_i$ are amenable to simpler interpretation, and modeling.[16] The $Đ_{ii}$ in eq 3 is the *self-exchange* coefficient that captures the correlation effects. The smaller the value of the self-exchange coefficient $Đ_{ii}$ with respect to the M-S diffusivity $Đ_i$, the stronger are the consequences of correlation effects, and we may consider the ratio $Đ_i/Đ_{ii}$ as a measure of the *degree* of correlations. The stronger the degree of correlations, the lower is the value of $D_{i,self}$ below that of $Đ_i$.

The normalized self-diffusivities $D_{i,self}/Đ_i(0)$ for *n*-alkanes in IRMOF-1 at 300 K are shown in Figure 6c. We note that $D_{i,self}/Đ_i(0)$ displays progressively sharper peaks as the chain length increases, consonant with the results presented in Figure 1.

Figure 6d compares the data on normalized self-diffusivities of nC6 in IRMOF-1 at various temperatures. We note that, as the temperature is increased, and T_R approaches unity, the peaks in the diffusivity values become shallower. For $T = 450$ K, there is no maximum and the maximum in the self-diffusivity of nC6 disappears, and $D_{i,self}$ shows a near-monotonic decrease with increased loading; at 450 K, the degree of clustering is very small because $T_R = 0.89$ is much closer to unity. Xue and Zhong[42] have reported similar results on the influence of temperature.

The Fick, or transport, diffusivity is related to the M-S diffusivity by the thermodynamic factor

$$D_i = Đ_i \Gamma_i \tag{4}$$

When no molecular clustering occurs, $1/\Gamma_i < 1$, and the hierarchy $D_i > Đ_i > D_{i,self}$, prevailing over the entire concentration range, typifies "normal" behavior for guest molecules in microporous structures. All three diffusivities converge to the same value at infinitely dilute loadings. This "normal" behavior is exhibited, for example, by CH_4 diffusion in IRMOF-1 at 300 K, significantly higher that its T_c value of 191 K and therefore no clustering occurs; see Figure 7a. In this "normal" behavior, the Fick $Đ_i$ increases with increased loading. One important consequence of this is that, for uptake of a single component within a microporous crystal, the adsorption kinetics is usually faster than the desorption kinetics.[10,43]

The situation changes dramatically for higher chain lengths with attendant clustering; see Figure 7b,c,d for data on C3, nC4, and nC5 in IRMOF-1. We note that, in the concentration ranges where $1/\Gamma_i > 1$, indicated by the shaded areas, the Fick diffusivity, D_i, can be lower than both the M-S diffusivity, $Đ_i$, and the self-diffusivity, $D_{i,self}$. Analogous results are obtained for alkane diffusivities in PCN-6′; details are provided in the Supporting Information accompanying this publication. Of particular interest is the minimum in the D_i at the concentration c_i corresponding to the maximum in the $1/\Gamma_i$ vs c_i in Figure 1. This minimum is

(42) Xue, C.; Zhong, C. *Chin. J. Chem.* **2009**, *27*, 472–478.

(43) Garg, D. R.; Ruthven, D. M. *Chem. Eng. Sci.* **1972**, *27*, 417–423.

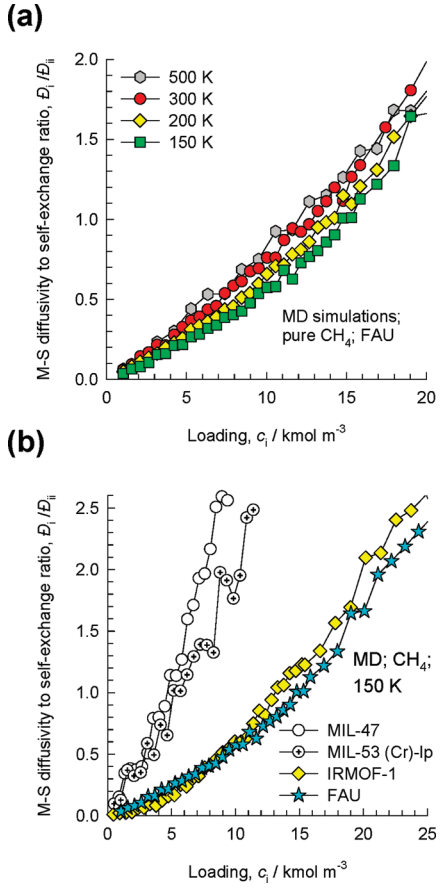

Figure 8. Ratio of the M-S diffusivity $Đ_i$ with respect to self-exchange coefficient $Đ_{ii}$ for (a) CH_4 diffusion in FAU at various temperatures. (b) CH_4 diffusion at 150 K in IRMOF-1, MIL-47, MIL-53(Cr)-lp, and FAU.

entirely analogous to the minimum observed in the experimental work of Chmelik et al.[26] for 2MB and neo-C5 diffusion in CuBTC. Direct experimental verification of $D_i < D_{i,\text{self}}$ when $1/\Gamma_i > 1$ is available in the recent work of Chmelik et al.[44] for methanol and ethanol diffusion in ZIF-8. In this case, the clustering of alcohol molecules is induced by hydrogen bonding, as we shall demonstrate in a subsequent publication.

When strong clustering occurs, the Fick $Đ_i$ decreases with increased loading for a range of concentrations, indicated by the shaded regions in Figures 7 . Within this concentration range, we should expect the desorption rate for uptake within a crystal to be higher than the adsorption rate .

Let us examine how clustering phenomena influences the ratio $Đ_i/Đ_{ii}$, quantifying the strength of correlations. Consider the data in Figure 8a on $Đ_i/Đ_{ii}$ for diffusion of CH_4 in FAU at 150 K, 200 K, 300 K, and 500 K. At any given T, the degree of correlations increases with increasing pore concentration c_i. This is because, as the loading within the pore increases, there are fewer vacant sites for the guest molecules to jump to. Consequently, the probability that a molecule has to revisit the site it had vacated is increased, and molecular jumps become increasingly correlated. At any given pore concentration c_i, the degree of correlations is lower as T is lowered below T_c. Clustering of CH_4 molecules has the effect of reducing the degree of correlations. As argued earlier, molecular clustering has the effect of increasing the availability of vacant sites. Consequently, the degree of correlations is decreased

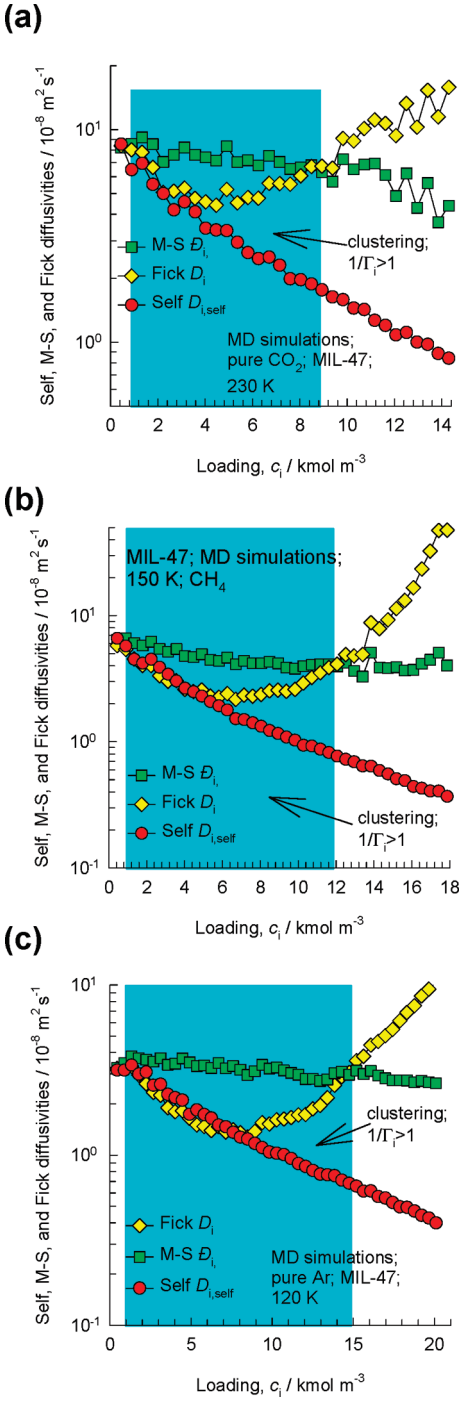

Figure 9. The loading dependences of the Maxwell-Stefan (M-S) diffusivity, $Đ_i$, Fick diffusivity, D_i, and the self-diffusivity, $D_{i,\text{self}}$ for (a) CO_2 diffusion in MIL-47 at 230 K, (b) CH_4 diffusion in MIL-47 at 150 K, and (c) Ar diffusion in MIL-47 at 120 K.

with increasing amounts of cluster formation. Analogous results are obtained for CO_2 and Ar diffusion and for every guest−host combination investigated; see Supporting Information for details.

Figure 8b compares the degree of correlations for CH_4 diffusion at 150 K in FAU, IRMOF-1, MIL-47, and MIL-53 (Cr). We note that, at any given pore concentration, c_i, the degrees of correlation are stronger in 1D channels. Consequently, $D_{i,\text{self}} \ll Đ_i$. This is illustrated in Figure 9 for CO_2, CH_4, and Ar diffusion in MIL-47 at temperatures T less than their corresponding T_c. We note that the Fick D_i does not fall below $D_{i,\text{self}}$ at any concentration. The important message to be derived from the results

(44) Chmelik, C.; Bux, H.; Caro, J.; Heinke, L.; Hibbe, F.; Titze, T.; Kärger, J. *Phys. Rev. Lett.* **2010**, *104*, 085902.

presented in Figures 7 and 9 is that, when clustering occurs, it is not essential that the Fick D_i is lower than the self-diffusivity $D_{i,self}$; it will be lower only for structures that do not exihibit strong correlations. The recent experimental works of Salles et al.[45,46] for CO_2 diffusion in MIL-47 and MIL-53(Cr)-lp at 230 K provides confirmation of the trends portrayed in Figure 9a. Their data show that $D_i < Đ_i$ in regions where $1/\Gamma_i > 1$, most likely caused by clustering.

For a fixed pore concentration c_i, we investigated the influence of temperature on the degree of correlations for a variety of guest−host combinations; a few typical results are shown in Figure 10. The ratio $Đ_i/Đ_{ii}$ decreases significantly at reduced temperatures $T_R = T/T_c$ below unity. For $T_R \gg 1$, the $Đ_i/Đ_{ii}$ appears to reach an asymptotic value suggesting that, for temperatures far in excess of T_c, the degree of correlations is T-independent; this conclusion was also reached in an earlier study.[47] Also shown in Figure 10a are the data for MFI; in this case, no influence of T on the degree of correlations is detected. The reason for this is that within the 0.56 nm pores of MFI the degree of clustering is negligibly small due to strong molecule−wall interactions.[22]

A reduction in the degree of correlation with reduction in temperature also implies that the self-diffusivity, $D_{i,self}$, will be relatively closer to the M-S diffusivity $Đ_i$ as T is reduced. Figure 11a,b presents the Arrhenius plots for both $D_{i,self}$ and $Đ_i$ of CO_2 and CH_4 in IRMOF-1 at a total loading of 60 molecules per unit cell, corresponding to $c_i = 7.12$ kmol m^{-3}. The activation energy of $D_{i,self}$ is consistently lower than that of corresponding $Đ_i$; this is a consequence of reduced correlations at lower T. Analogous results are obtained for several other guest−host combinations; see Supporting Information.

It is not uncommon in the published literature to compare activation energies obtained by different measurement techniques such as ZLC, PFG NMR, and QENS.[48] Such a comparison is not strictly valid, because PFG NMR and QENS yield data on activation energies of the self-diffusivities, whereas those obtained from ZLC are related to the M-S diffusivities. The concept of activation energy should only be applied to zero-loading diffusivities, as has been stressed in an earlier publication.[47]

When the degree of clustering is severe, non-Arrhenius behavior may result. This is illustrated in Figure 11c,d for diffusion of nC5 and nC6 in IRMOF-1 for a loading of 30 molecules per unit cell. Neither the M-S nor the self-diffusivity data is susceptible to a linear Arrhenius plot for these molecules. Molecular clustering is also the cause of the non-Arrhenius temperature dependence of diffusivity of water in FAU and MFI;[49] in this case, the clustering of water molecules is the result of hydrogen bonding.

5. Influence of Clustering on Diffusion in Binary Mixtures

The discussions on clustering influence on mixture diffusion are best understood within the framework of the M-S equations,

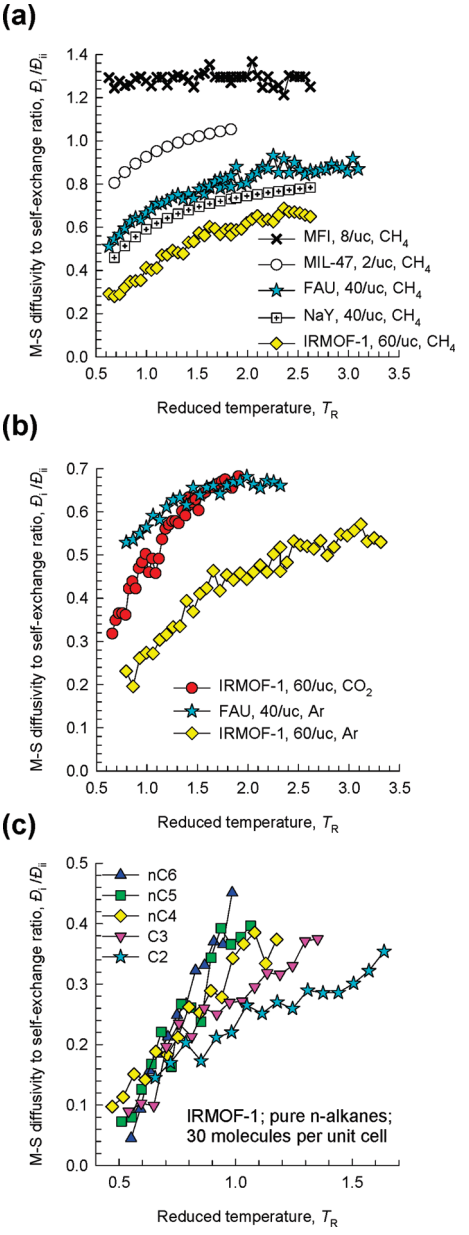

Figure 10. Ratio of the M-S diffusivity $Đ_i$ with respect to self-exchange coefficient $Đ_{ii}$ as a function of the reduced temperature for diffusion of (a) CH_4, (b) CO_2, Ar, and (c) linear alkanes in a variety of zeolites and MOFs.

which for binary mixtures takes the form

$$-\frac{c_i}{RT}\nabla\mu_i = \sum_{\substack{j=1\\ j\neq i}}^{2}\frac{x_j N_i - x_i N_j}{Đ_{ij}} + \frac{N_i}{Đ_i} \quad i = 1,2 \tag{5}$$

where x_i represents the component mole fractions of the adsorbed phase within the microporous structures

$$x_i = c_i/c_t \quad i = 1,2 \tag{6}$$

The coefficients $Đ_i$ are identifiable with the corresponding M-S diffusivity for unary diffusion; these are influenced by clustering in the manner discussed in the foregoing section. The $Đ_{12}$ are exchange coefficients representing interaction between component 1 and component 2. At the molecular level, the $Đ_{12}$ reflect how the facility for transport of species 1 correlates with that of

(45) Salles, F.; Jobic, H.; Ghoufi, A.; Llewellyn, P. L.; Serre, C.; Bourrelly, S.; Férey, G.; Maurin, G. *Angew. Chem., Int. Ed.* **2009**, *48*, 8335–8339.
(46) Salles, F.; Jobic, H.; Devic, T.; Llewellyn, P. L.; Serre, C.; Férey, G.; Maurin, G. *ACS Nano* **2010**, *4*, 143–152.
(47) Krishna, R.; van Baten, J. M. *Microporous Mesoporous Mater.* **2009**, *125*, 126–134.
(48) Jobic, H.; Kärger, J.; Krause, C.; Brandani, S.; Gunadi, A.; Methivier, A.; Ehlers, G.; Farago, B.; Haeussler, W.; Ruthven, D. M. *Adsorption* **2005**, *11*, 403–407.
(49) Fleys, M.; Thompson, R. W.; MacDonald, J. C. *J. Phys. Chem. B* **2004**, *108*, 12197–12203.

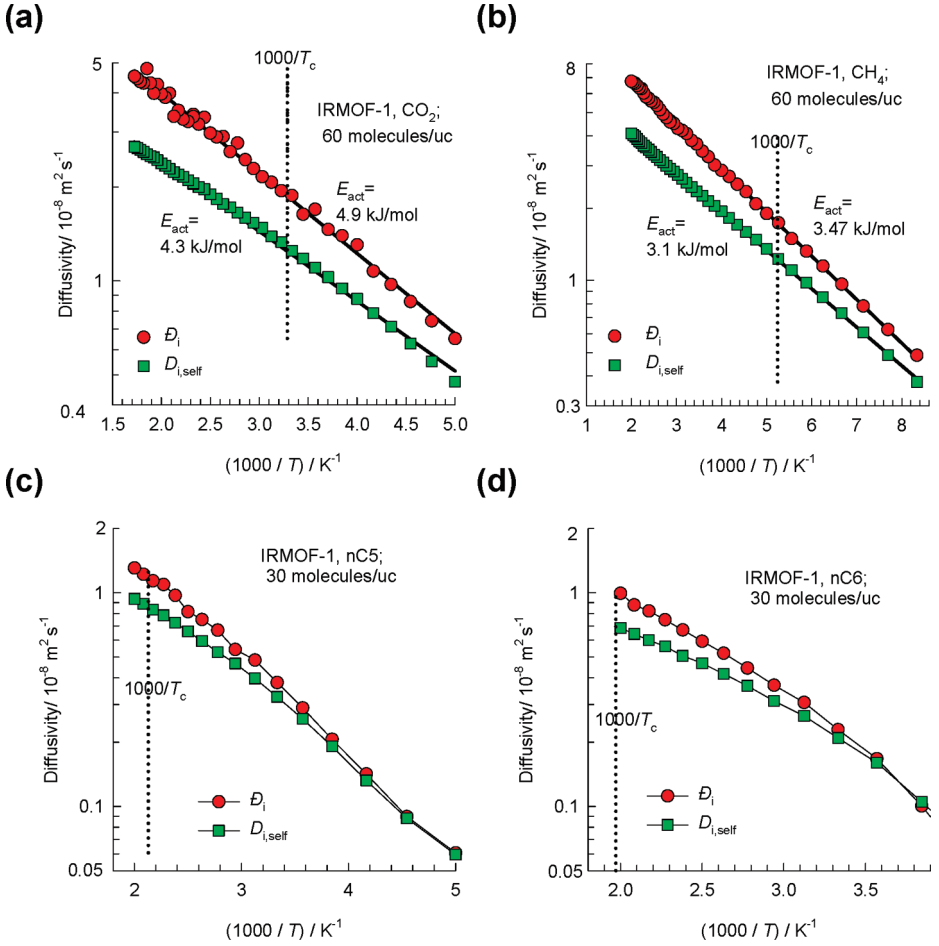

Figure 11. Arrhenius plots for MD simulated values of self-diffusivity $D_{i,self}$ and M-S diffusivity Đ$_i$ of (a) CO_2, (b) CH_4, (c) nC5, and (d) nC6 in IRMOF-1.

species 2. Conformity with the Onsager reciprocal relations prescribes

$$Đ_{12} = Đ_{21} \tag{7}$$

The exchange coefficient Đ$_{12}$ is influenced by correlation effects in much the same way as the exchange coefficients Đ$_{ii}$ of the constituent pure species. On the basis of extensive MD data, the following interpolation formula, based on the Vignes[50] model for diffusion in liquid mixtures, has been proposed in our previous work that was largely restricted to temperatures in excess of T_c.[16,28]

$$Đ_{12} = (Đ_{11})^{x_1}(Đ_{22})^{x_2} \tag{8}$$

In using eq 8, the Đ$_{11}$ and Đ$_{22}$ have to be evaluated at the total mixture loading $c_t = c_1 + c_2$. We now investigate whether the interpolation formula holds when T is lower than the T_c of at least one of the components in the mixture. Figure 12a presents data on self-exchange coefficient Đ$_{11}$, along with the binary exchange coefficient Đ$_{12}$ for diffusion of CH_4−*n*-alkane equimolar mixtures in IRMOF-1 at 300 K. We note that the Vignes interpolation formula (eq 8) provides a good estimation of Đ$_{12}$ even though the $T < T_c$ of the partner molecules of CH_4. Validation of eq 8 is also obtained for CH_4−CO_2 mixture diffusion in IRMOF-1 at 200 K and 300 K (cf. Figure 12b).

For a fixed total loading $c_t = c_1 + c_2 = 60$ molecules per unit cell, the Đ$_{12}$ for CH_4−CO_2 mixture diffusion in IRMOF-1 as determined for a range of temperatures and the results are presented in Figure 12c, along with the corresponding self-exchange Đ$_{ii}$. The Vignes interpolation formula in eq 8 is seen to provide a reasonable estimate of Đ$_{12}$ over the entire temperature range. The success of the Vignes interpolation formula (eq 8) is due to the fact that the self-exchange coefficients Đ$_{11}$ and Đ$_{22}$ properly account for variation of the clustering tendency of the constituents species with varying T.

Correlation effects in mixture diffusion have the effect of slowing down the more mobile species (say, species 1), and speeding up the tardier one (say, species 2). The ratio of self-diffusivities can be derived from the M-S equations[16]

$$\frac{D_{1,self}}{D_{2,self}} = \frac{\left(\frac{1}{Đ_2}+\frac{x_1}{Đ_{12}}+\frac{x_2}{Đ_{22}}\right)}{\left(\frac{1}{Đ_1}+\frac{x_2}{Đ_{12}}+\frac{x_1}{Đ_{11}}\right)} \tag{9}$$

A reduction in the degree of correlations will have the effect of increasing the ratio $D_{1,self}/D_{2,self}$. This is demonstrated in Figure 13 for CH_4−C3, and CH_4−CO_2 mixture diffusion in IRMOF-1. We note that with increasing temperature the ratio of the self-diffusivity of the more mobile species (1) to that of the tardier species (2) is decreased. We also note from Figure 13c

(50) Vignes, A. *Ind. Eng. Chem. Fundamentals* **1966**, *5*, 189–199.
(51) Myers, A. L.; Prausnitz, J. M. *A. I. Ch. E. J.* **1965**, *11*, 121–130.
(52) Krishna, R.; Paschek, D.; Baur, R. *Microporous Mesoporous Mater.* **2004**, *76*, 233–246.

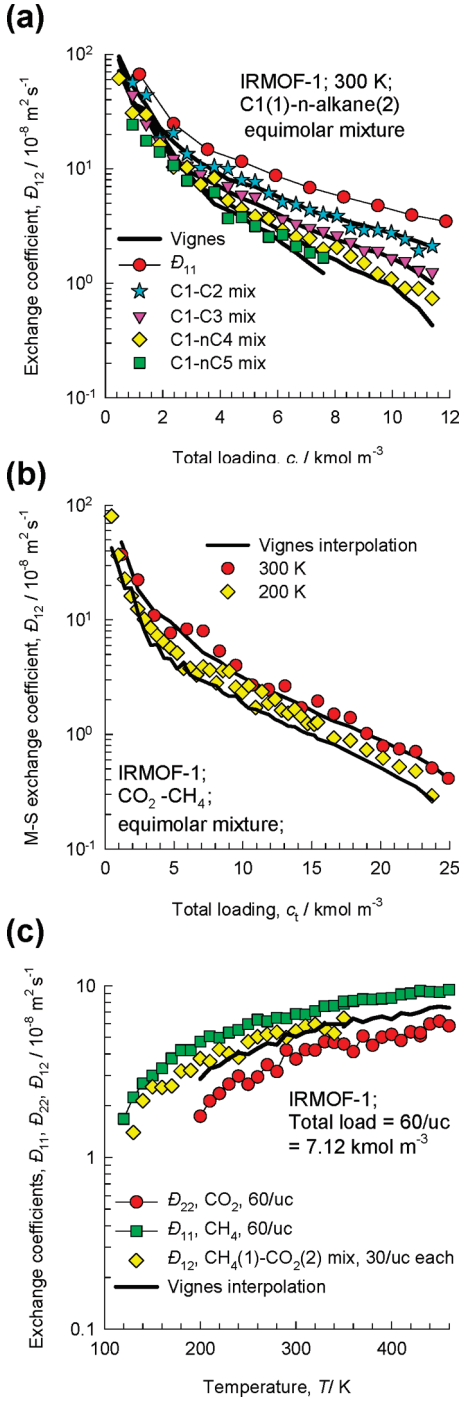

Figure 12. Binary exchange coefficient $Đ_{12}$ for mixture diffusion. (a) Diffusion of $CH_4(1)-n$-alkane(2) equimolar mixtures in IRMOF-1 at 300 K. (b) Diffusion of $CH_4(1)-CO_2(2)$ equimolar mixtures in IRMOF-1 at 200 K and 300 K. (c) Diffusion of $CH_4(1)-CO_2(2)$ equimolar mixtures in IRMOF-1 at various temperatures at a loading of 60 molecules per unit cell, corresponding to $c_i = 7.12$ kmol m^{-3}. The continuous solid line represents the calculations using the Vignes interpolation formula (eq 8).

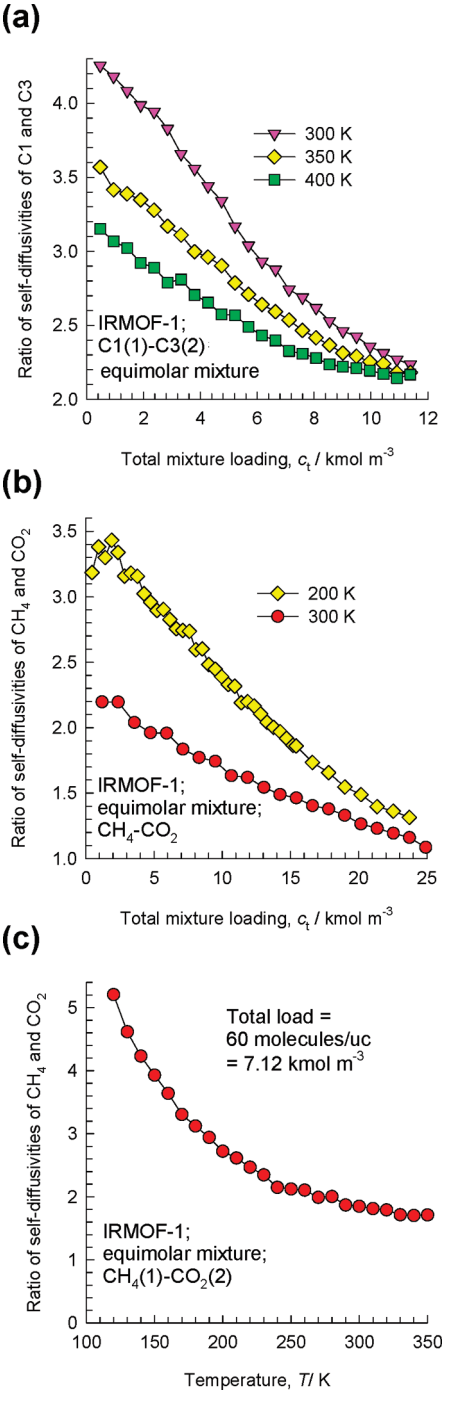

Figure 13. Ratio of the self-diffusivity of the more mobile species (1) to that of the tardier species (2) for diffusion of (a) $CH_4(1)-$C3-(2), (b,c) $CH_4(1)-CO_2(2)$ equimolar mixtures in IRMOF-1.

that, at temperatures far in excess of T_c of either component, $D_{1,\text{self}}/D_{2,\text{self}}$ reaches an asymptotic value, consistent with the conclusion drawn earlier that correlations become T-independent at high enough temperatures.

The self-diffusivities, $D_{i,\text{self}}$, of equimolar nC4/iC4 mixtures in IRMOF-1 and PCN-6′ at 300 K display a maximum at loadings corresponding to the maximum in the respective $1/\Gamma_i$ vs c_i data for pure components; see Figure 14a,b. The observed maximum in Figure 14b for nC4/iC4 mixture diffusion in PCN-6′ is consistent with the results of Babarao et al.;[21] our work clearly shows that molecular clustering is the root cause. A further interesting feature to note in Figure 14b is the minimum within the range $0 < c_t < 1.2$ kmol m^{-3}. The reasoning can be traced to the corresponding minima in the pure component $1/\Gamma_i$ vs c_i data (cf. Figure 3b), caused by the preferential location of C4 isomers within the octahedral pockets at low concentrations c_i.

Babarao et al.[21] also performed MD simulations for a ternary nC5/2MB/neo-C5 mixture diffusion in PCN-6′ and found maxima for the $D_{i,\text{self}}$ of each component, with the hierarchy of

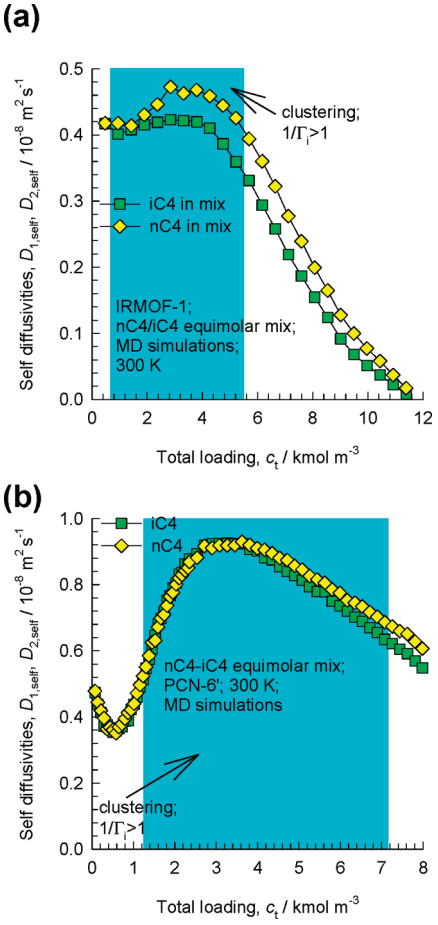

Figure 14. Self-diffusivities, $D_{i,self}$, of equimolar nC4/iC4 mixtures in (a) IRMOF-1 and (b) PCN-6′ at 300 K.

magnitudes nC5 > 2MB > neo-C5, entirely consistent with the hierarchy of the pure component $1/\Gamma_i$ vs c_i data presented in Figure 3e. Their diffusivity results are rationalized by our current work and are traceable to differences in the degree of clustering of linear and branched C5 isomers; cf. Figure 3e.

A qualitative appreciation of clustering can be obtained by viewing the animations of MD simulations of diffusion of a variety of guest−host combinations; these are available as Supporting Information accompanying this publication.

6. Conclusions

The important message that emerges from the investigations reported here is that the adsorption and diffusion characteristics in zeolites and MOFs, with pore sizes larger than 0.75 nm, are strongly influenced by molecular clustering phenomena that manifests at temperatures below T_c. Specifically, we can draw the following set of conclusions. (1) For adsorption of *n*-alkanes at any given temperature, clustering phenomena is of increasing importance with increasing chain length. As a consequence, the inverse thermodynamic factor $1/\Gamma_i$ exceeds unity for a range of concentrations c_i; in this concentration range the M-S diffusivity, $Đ_i$, shows a maximum. (2) When the extent of clustering is severe, and $1/\Gamma_i \gg 1$, the Fick diffusivity, D_i, can be lower than the self-diffusivity, $D_{i,self}$, for a range of concentrations. (3) For C4, C5, and C6 alkane isomers, the linear molecule has the highest T_c, and consequently exhibits the highest degree of clustering. Such differences in the degree of clustering can be exploited to effect isomer separation. (4)The adsorption selectivity in mixtures is significantly enhanced in favor of the component with a higher degree of clustering. (5) Clustering phenomena provide an explanation for the curious maxima observed by Babarao et al.[21] for the self-diffusivities of C4 and C5 isomers in PCN-6′. (6) Correlation effects are reduced with increased degree of clustering and are dictated by the value of the reduced temperature T_R. The smaller T_R goes below unity, the lower the strength of correlations. Conversely, when $T_R \gg 1$, correlation effects are practically *T*-independent. (7) When the degree of clustering is severe, the *T*- dependence of the diffusivities may exhibit non-Arrhenius behavior. (8) Increased degree of clustering has the consequence of increasing the diffusion selectivity for mixture diffusion. (9) The interpolation formula in eq 8 is found to be applicable also in cases where one or both of the components in the mixture form clusters. (10) Since both adsorption and diffusion selectivities are significantly increased with degree of clustering, the permeation selectivity of mixtures in membrane separations can be improved by an optimum choice of temperature.

The current work has highlighted a variety of peculiar adsorption and diffusion characteristics induced by cluster formation for operations below subcritical temperatures. Many detailed mechanistic aspects deserve further investigation. These include determination of cluster sizes, cluster lifetimes, cluster disintegration, and regrouping phenomena. These aspects will be addressed in a follow-up publication, that will also investigate adsorption of polar molecules such as water and alcohols for which cluster formation is induced by hydrogen bonding.

Acknowledgment. R.K. acknowledges the grant of a TOP subsidy from The Netherlands Foundation for Fundamental Research (NWO−CW) for intensification of reactors. R.K. acknowledges helpful suggestions from Dr. D. Dubbeldam.

Supporting Information Available: Details of the CBMC and MD simulation methodologies, details of the microporous structures (unit cell dimensions, accessible pore volume), pore landscapes, description of the force fields used, simulation data on isotherms, and diffusivities. Animations of MD simulations for diffusion of (a) nC4, nC5, nC6 diffusion in IRMOF-1, and PCN-6′ at 300 K and (b) CH_4−CO_2 mixtures in IRMOF-1, AFI, and MIL-47 at 200 K. These animations provide some qualitative indication of clustering phenomena in mixtures. This material is available free of charge via the Internet at http://pubs.acs.org.

Glossary

b_i	dual-Langmuir-Sips constant for species *i*, Pa^{-vi}
c_i	concentration of species *i*, mol m^{-3}
$c_{i,sat}$	saturation capacity of species *i*,mol m^{-3}
c_t	total concentration in mixture, mol m^{-3}
D_i	Fick diffusivity of species *i*, m^2 s^{-1}
$D_{i,self}$	self-diffusivity of species *i*, m^2 s^{-1}
$Đ_{ii}$	self-exchange coefficient, m^2 s^{-1}
$Đ_i$	M-S diffusivity, m^2 s^{-1}
$Đ_i(0)$	zero-loading M-S diffusivity, m^2 s^{-1}
$Đ_{12}$	binary exchange coefficient defined by eq 5, m^2 s^{-1}
f_i	fluid phase fugacity of species *i*, Pa
N_i	molar flux of species *i*, based on pore space, mol m^{-2} s^{-1}
R	gas constant, 8.314J mol^{-1} K^{-1}
T	absolute temperature,K
T_c	critical temperature, K
T_R	reduced temperature, K
V_p	pore volume per mass of framework, cm^3 g^{-1}

x_i mole fraction of species i based on loading within pore, dimensionless

Greek letters

Γ_i thermodynamic factor, dimensionless
μ_i molar chemical potential, J mol^{-1}
ν_i exponent in the dual-Langmuir-Sips isotherm, dimensionless
θ_i fractional occupancy of i, dimensionless
Θ_i loading of i, molecules per unit cell

Subscripts

A,B referring to adsorption sites Aand B
c critical parameter
i referring to component i
R reduced parameter
sat referring to saturation conditions
t referring to total mixture

Vector Notation

∇ gradient operator